EFFECTS OF CRAB CAVITIES' MULTIPOLE CONTENT IN AN ELECTRON-ION COLLIDER[*]

A. Castilla[1,2,3][†], V. S. Morozov[2], T. Satogata[1,2], J. R. Delayen[1,2].
[1]Center for Accelerator Science, Old Dominion University, Norfolk, VA 23529, USA.
[2]Thomas Jefferson National Accelerator Facility, Newport News, VA 23606, USA.
[3]Universidad de Guanajuato (DCI-UG), Departamento de Fisica, Leon, Gto. 37150, Mex.

Abstract

The impact on the beam dynamics of the Medium Energy Electron-Ion Colider (MEIC) due to the multipole content of the 750 MHz crab cavity was studied using thin multipole elements for 6D phase space particle tracking in ELEGANT. Target values of the sextupole component for the cavity's field expansion were used to perform preliminary studies on the proton beam stability when compared to the case of pure dipole content of the rf kicks. Finally, important effects on the beam sizes due to non-linear components of the crab cavities' fields were identified and some criteria for their future study were proposed.

INTRODUCTION

Strong interest has been generated among the nuclear physics comunity for building an Electron-Ion Collider with a broad range of center of mass energy ($\sqrt{s} = 20 - 70$ GeV) and high luminosities ($\sim 10^{34}$cm^{-2}s^{-1}) per interaction point (IP) [1]. In order to have a full acceptance detector, a relatively large crossing angle (50 mrad) of the colliding beams has to be introduced. Then, the only way to reach the high luminosity required is to implement crab crossing correctors. A crab cavity suitable for this application is an rf deflector that operates at the transverse voltages needed to restore this angle for both protons up to 150 GeV and electrons up to 20 GeV. The design proposed as crab cavity candidate for the MEIC at Jefferson Lab is an rf dipole geometry that operates on a fundamental TE-like mode. The exercises performed in the present paper use the former MEIC baseline frequency of 750 MHz to analyze the effect of the sextupole component of the rf kick given by such a cavity on the proton bunches at 60 GeV as a case study, even when the baseline frequency of collision may be changed, the methods developed here can easily be implemented for different beam energies and frequencies without major difficulties.

ANALYTICAL CONSIDERATIONS

If we treat the horizontal crabbing of the bunch as a chirp in x, then we can express the change in emittance due to this chirp [2] as:

$$\frac{\Delta \epsilon_x}{\epsilon_x} = \frac{\sqrt{\sigma_{x'}^2 + \sigma_{\Delta x'}^2}}{\sigma_{x'}^2} - 1. \quad (1)$$

Using a definition of the thin-lense rf multipole transverse kick, such as:

$$\begin{aligned} \Delta x' &= \frac{\Delta p_x}{p_z} \\ &\approx \mathcal{V}_0 \left(b_1 + b_3 \left(x^2 - y^2 \right) + ... \right) \cos(\phi). \quad (2) \end{aligned}$$

Where $\mathcal{V}_0 \equiv \frac{eV_x}{p_z mc^2 k}$, with V_x as the total crabbing voltage, p_z the particle momentum, $k = \frac{\omega_{rf}}{\beta c}$, b_1 and b_3 are the dipole and sextupole coefficients respectively, and $\phi = 270^o$ as the rf phase with respect to the bunch centroid.

Then we can write:

$$\sigma_{\Delta x'} \approx \frac{\mathcal{V}_0 b_3}{2} \sqrt{\sigma_{x^2}^2 + \sigma_{y^2}^2}, \quad (3)$$

thus, using Eqns. 1 and 3 we express in this notation the change on emittance per turn as:

$$\frac{\Delta \epsilon_x}{\epsilon_x} = \frac{\sqrt{\sigma_{x'}^2 + \frac{\mathcal{V}_0^2 b_3^2}{4} \left(\sigma_{x^2}^2 + \sigma_{y^2}^2 \right)}}{\sigma_{x'}} - 1. \quad (4)$$

Which shows that the change in the emittance will depend on the transverse second momenta of the bunches and the sextupole component. This shows how geometrically the sextupole content on the crabbing kicks may have repercussions on the beam luminosity or even the beam lifetime. For this reason we will compare the cases with a pure dipole kick to some cases where there is a sextupole component to the rf kick to look for possible resonances or relative stability conditions for the crab cavities' operation.
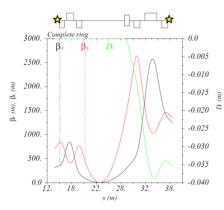
TRACKING METHODS

In this section we will first describe the simplifications made to the lattice to focus our numerical studies on the section of the interaction region (IR), proposing a linear map for the proton storage ring that properly accounts for the transverse and longitudinal dynamics of the machine, leaving the IR description as a separate block. Secondly, we will discuss the tracking elements and basic calculations performed in different sections of the IR.

Modeling the Lattice

As mentioned above, we used linear maps for the 6D dynamics of the entire proton storage ring, excluding the interaction region as seen in the schematic on Fig. 1, while the interaction region and its transverse Twiss functions are described in Fig. 2

Figure 1: Conceptual diagram of the tracking approach, the ring is described as a linear map, while the interaction region is constituted by several single elements.

Figure 2: Interaction region optics, where the yellow stars represent the crab cavity locations.

Particle Tracking

All the 6D phase space tracking was done using ELE-GANT, the linear map was placed at the end of the IR as described in Figs. 1 and 2. The final focusing blocks (FFBs) at each side of the IP were described using elements such as QUAD, CSBEND, and DRIFT [3], while for the crab cavities we used zero-length multipole rf kicker (MRFDF) elements at zero crossing ($\phi = 270^o$). In this way and for the purpose of the present study, we reduced the number of non-linear contributions to isolate the effects of the higher order multipole contents of the cavities.

We tracked for a 1000 turns a uniform ellipse distribution of protons with the parameters described in Table. 1

Table 1: Parameters of the Employed Proton Distribution

Parameter	Value	Units
Central momentum	60	GeV
Number of particles	10^4	–
$\epsilon_{N,x}$	0.35	mm-mrad
$\epsilon_{N,y}$	0.07	mm-mrad
$\sigma_{\Delta p/p}$	3.0×10^{-4}	–
σ_s	10^{-2}	m

The linear map for the longitudinal dynamics was constructed following [4] for a fractional synchrotron tune of $\nu_s = 0.01$. Fig. 3 (a) shows the longitudinal phase space coming out of the IR for the last 20 of a 1000 turns of the lattice without the crab cavities being turned on.
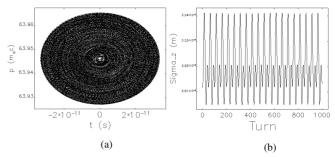

Figure 3: Longitudinal phase space, plotted for the last 20 of a 1000 turns without crab cavities (a), and longitudinal beam size showing oscillations in the order of the numerical errors (0).

RESULTS

Pure Dipole Case

We set the corresponding value of $\mathcal{V}_{0,C1}$ for the zero-length dipole kick at the first cavity location to crab horizontally the bunch at the IP by 25 mrad, without any higher order multipole contribution. Another zero-length dipole kick was set at the second crab cavity location with a magnitude of $\mathcal{V}_{0,C2} = \sqrt{\frac{\beta_x^{C1}}{\beta_x^{C2}}}\mathcal{V}_{0,C1}$, which would completely cancel the effects of the first crab on the bunch, only for the case of on exact $n\pi$ phase advance between the crab cavities. In this case, β_x^{C1} and β_x^{C2} are the horizontal beta functions at the locations of the first and second crab cavities, respectively. Any multipole contribution, higher than the dipole, was set to zero for this first step of the work.

After setting the conditions above described, we tracked the particles for a 1000 turns, Fig. 4(a) shows the crabbed bunch at the IP location for the last 3 of a 1000 turns, while 4(b) shows the calculated crabbed angle for the 1000 turns, calculated according to Eqn. 5

$$\tan(\theta_c) \approx \theta_c = \frac{\langle xz \rangle}{\langle z^2 \rangle} = \frac{\langle xt \rangle}{\beta c \langle t^2 \rangle} \tag{5}$$

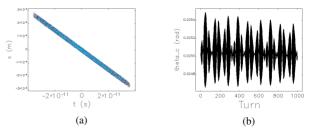It can be noted from Fig. 4 (b) how the effective crabbed

Figure 4: Crabbed 60 GeV proton bunches at IP (a) and calculated crabbed angle (b), using a pure dipole contribution from the rf cavities.

angle of the bunches at the IP oscillates around the desired value by roughly ± 0.5 mrad with different convoluted frequencies, this is due to both synchro-betatron motions and

small relative phase advance errors between the crab cavities.

The behavior of the transverse and longitudinal beam sizes as a function of the number of turns, gives an insight to the θ_c variations at the IP. From Fig. 5 (a), (b), and (c) can be noted the associated betatron and synchrotron oscillations, and from (d) it is evident that a residual x-z angle at the location of the first crab will translate in an error of the total crabbed angle at the IP, this residual error appears to be stable for the studied range (1000 turns) for the case of pure dipole rf kick and could presumably be accounted for an exchange of horizontal and longitudinal emittances (compared with Fig. 3 (b)). However, more detailed studies need to be performed to determine the real scope of this effects and their range of stability, which would establish important criteria for the high luminosity operation of the machine.
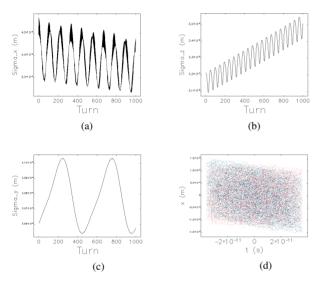
(a)

(b)

(c)

(d)

Figure 5: Beam sizes for x (a), z (b), and y (c) for the case of a pure dipole rf kick. (d) shows a residual x-z angle of the bunch at the entrance of the first cavity.

Adding a Sextupole Contribution

For this case we added a contribution consistent with the characteristic range of sextupole strength for the 750 MHz rf dipole [5] and calculated the crabbed angle at IP and the beam sizes at the first crab cavity location for a 1000 turns (see Fig. 6)

From Fig. 6 (a) we can observe a noticeable damping of the amplitude of the crabbed angle variation after 1000 turns compared to Fig. 4, as well as variations of the transverse and longitudinal beam sizes (b), (c), and (d) with the difference that with the introduction of a non-linear (sextupole) contribution, both the transverse beam sizes seem to be involved in emittance exchange process. Apparently, the relative stability for the case of pure dipole contributions and the case of including a small sextupole contribution to the crabbing rf kicks, for the range studied (1000 turns), does not change radically. However, it is important to perform de-
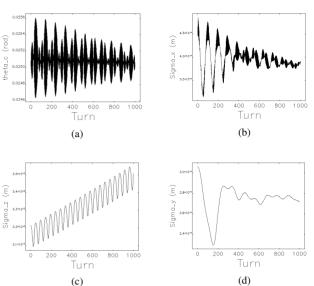
(a)

(b)

(c)

(d)

Figure 6: For the case of a small sextupole contribution: the crabbed angle at IP (a), the longitudinal beam size (growing at similar rate than for the pure dipole case) (c), and both horizontal and vertical beam sizes (b) and (d), respectively.

not change radically. However, it is important to perform detailed studies of these effects to avoid resonances that could compromise the beam emittances.

CONCLUSIONS

The lattice model proposed for particle tracking studies hereby presented has proven to properly describe the transverse and longitudinal dynamics of the MEIC proton storage ring. Also, rf crab cavities were succesfully implemented to account for a relative 25 mrad crabbing angle of the 60 GeV proton bunches at the IP, showing effects of small phase advance errors between the crab cavities are consistent with previous analytical calculations. The stability of the longitudinal beam size growth due to the induced emittance exchange needs to be studies for a sufficient amount of turns, both for the case of pure dipole and sextupole components to ensure stable operation conditions and to establish multipole budgets for the rf crab cavities on the MEIC.

REFERENCES

[1] S. Abeyratne, et al, "Science Requirements and Conceptual Design for a Polarized Medium Energy Electron-Ion Collider at Jefferson Lab", JLAB-ACC-12-1619 (2012).

[2] M. Borland, "Simulation and Analysis of Using Deflecting Cavities to Produce Short X-ray Pulses with the Advanced Photon Source", PRSTAB 8, 074001 (2005).

[3] M. Borland, "User's Manual for ELEGANT", Version 27.1.0 (2015).

[4] J. Quiang, et al, "Strong-Strong Beam-Beam Simulation Using a Green Function Approach", PRSTAB 5, 104402 (2002).

[5] A. Castilla and J.R. Delayen, in Proceedings of LINAC 2014, Geneva, Switzerland. p. 326 (2014).